

# Periosteal reaction-like lesions at the cranial aspect of the humeral diaphysis have a high prevalence in older, large breed dogs and may represent entheses of the superficial pectoral muscles

Mareike-Kristin Nickel<sup>1</sup>  | Lisa Schikowski<sup>1</sup> | Carsten Staszky<sup>2</sup> | Sebastian Schaub<sup>1</sup>

<sup>1</sup>Department of Veterinary Clinical Sciences, Small Animal Clinic – Surgery, Faculty of Veterinary Medicine, Justus-Liebig-University Giessen, Giessen, Germany

<sup>2</sup>Institute of Veterinary Anatomy, Histology and Embryology, Faculty of Veterinary Medicine, Justus-Liebig-University Giessen, Giessen, Germany

## Correspondence

Mareike-Kristin Nickel, Department of Veterinary Clinical Sciences, Small Animal Clinic – Surgery, Faculty of Veterinary Medicine, Justus-Liebig-University Giessen, Frankfurter Strasse 114, 35392 Giessen, Germany.  
Email: [mareike.k.nickel@vetmed.uni-giessen.de](mailto:mareike.k.nickel@vetmed.uni-giessen.de)

## Abstract

Authors have commonly observed lamellar periosteal new bone formation at the cranial aspect of the humeral diaphysis in mediolateral radiographs of the humerus for large breed dogs with no evidence of pain or lameness. The aim of this retrospective, analytical study was to investigate the appearance and prevalence of “humeral periosteal reaction-like lesions” (HPRL) in dogs and identify any predispositions. Mediolateral radiographs of humeri were evaluated and the presence and extent of “humeral periosteal reaction-like lesions” at the cranial aspect of the humerus were recorded. Macroscopic and histological examination of the humeri were performed for one dog with HPRL. A total of 2877 mediolateral radiographs of 1727 dogs were included and focal or extended periosteal reaction-like lesions were found in 643 humeri of 387 dogs. Body weight  $\geq 30$  kg and age  $\geq 7$  years had a statistically significant, positive effect ( $P < 0.001$ ) on the presence of HPRL. German Shepherd dogs and Rottweilers were overrepresented in the group with HPRL ( $P < 0.01$ ). At the level of the HPRL, the enthesis of the superficial pectoral muscles (M. pectoralis descendens and M. pectoralis transversus) to the Crista tuberculi majoris and Crista humeri were macroscopically and histologically identified. The authors propose that higher mechanical loads to the enthesis in large breed dogs may lead to physiological, age-related remodeling processes of the muscular attachment. The finding should not be confused with a pathological condition such as bone neoplasia.

## KEYWORDS

anatomy, crest of the major tubercle, dog, periosteal reaction, radiography

**Abbreviations:** ECVDI, European College of Veterinary Diagnostic Imaging; HPRL, humeral periosteal reaction-like lesion.

This is an open access article under the terms of the [Creative Commons Attribution](https://creativecommons.org/licenses/by/4.0/) License, which permits use, distribution and reproduction in any medium, provided the original work is properly cited.

© 2022 The Authors. *Veterinary Radiology & Ultrasound* published by Wiley Periodicals LLC on behalf of American College of Veterinary Radiology.

## 1 | INTRODUCTION

Radiographic studies of the extremities are a key component of the clinical workup of front limb lameness in dogs. Interpretation of radiographic findings should integrate the patient's signalment, history, and clinical examination. Severity of lameness may not be correlated with severity of radiographic findings, as has been previously reported for young dogs with panosteitis.<sup>1</sup> Furthermore, radiographic changes in early stages of disease lag behind clinical signs or the extent is underestimated.<sup>2,3</sup> Radiography has a poor sensitivity for the detection of osteolytic lesions, as bone destruction is only visible when 30–50% of the bony substance is resorbed.<sup>4</sup> Knowledge of the normal anatomy and anatomic variants is crucial for radiologists and clinicians to correctly classify radiographic findings.

The authors of this study have commonly observed a smooth to mildly irregular bony double contour at the cranial aspect of the proximal and mid-diaphysis of the humerus in large breed dogs, without clinical signs of lameness or pain localized to the diaphysis of the humerus. The bony double contour resembles a lamellar periosteal reaction and is further referred to as a "humeral periosteal reaction-like lesion (HPRLL)". Periosteal reactions are the result of cortical bone reactivity to one or more stimuli, including neoplasia, trauma, infection, metabolic (e.g. panosteitis) or idiopathic bone diseases (e.g. metaphyseal osteopathy, hypertrophic osteopathy).<sup>5</sup> Irritation and elevation of the periosteum leads to periosteal new bone formation. The type and appearance of periosteal reactions can reveal the extent of an underlying process and help to compile a list of differential diagnoses.<sup>6</sup> Lamellar periosteal reactions are categorized as benign and are formed by subperiosteal exudate, cells, or hematoma, lifting the periosteum.<sup>4</sup> The formed space is consecutively filled with new bone material, resulting in a continuous, straight, or undulating mineral opaque line at bone surfaces. The HPRLL observed by the authors of this study are regarded as an incidental finding in dogs without signs of pain or causes of lameness attributed to a pathology of the humerus.

According to our conscientious review of literature, these HPRLL have not yet been described in veterinary literature. The purpose of this study was to describe the radiographic appearance and prevalence of HPRLL and identify any predisposition. Our first hypothesis was that the prevalence of these changes would be higher in large breed dogs and in dogs of greater age. Our second hypothesis was that HPRLL would represent a variation of the normal anatomy of the humerus and would not be associated with any underlying bone or soft tissue pathology.

## 2 | MATERIALS AND METHODS

### 2.1 | Selection and description of subjects

This was a retrospective, analytical study. All canine humeral radiographs acquired during the period of January 2010 to June 2021 at the Small Animal Clinic for Surgery of the Justus-Liebig University in

Giessen were retrieved from the hospital's patient database. The study protocol was approved by the head of Small Animal Clinic of Justus-Liebig University Giessen. Due to the retrospective character of the study, ethical approval was not required. Radiographs were screened by a first-year and a second-year European College of Veterinary Diagnostic Imaging (ECVDI) resident (M.N. and L.S.) under supervision of a board-certified specialist in veterinary diagnostic imaging (S.S. ECVDI). For inclusion in the current study, radiographs had to meet the following criteria: at least the proximal half of the humerus in the mediolateral projection had to be available, additional views were not mandatory for inclusion. Exclusion criteria were the presence or report of benign or malignant bone or soft tissue lesions at the level of the diaphysis or metaphysis of the humerus, humeral fracture proximal to the humeral condyles, pain on palpation of the humerus diaphysis and metaphyses according to the medical records, depiction of less than the proximal half of the humerus, or radiographic quality considered inadequate for the purpose of assessing the bone. Lame dogs were not in general excluded from the study.

### 2.2 | Data recording and analysis

#### 2.2.1 | Medical record review

All radiographs enrolled were obtained for breeding purposes or in the context of clinical investigations like front limb lameness after an indication had been set by the responsible veterinarian. Signalments and clinical characteristics of included dogs were retrieved from the medical records available in the hospital's patient database by a first- and a second-year ECVDI resident (M.N. and L.S.). The following data were recorded if available: breed, age, sex, weight, and information from the orthopedic examination. Decisions were based on consensus opinions.

#### 2.2.2 | Radiographic analyses

Radiographs were reviewed and graded by the same first-year and second-year ECVDI residents (M.N. and L.S.) using an image analysis workstation with dedicated Dicom viewing software (iMac Retina 5K, 2015, 27 inch, Apple, California; Horos version 3.3; [www.horosproject.org](http://www.horosproject.org)). Window width, window level, and magnification could be adjusted according to the personal preferences of the reviewers. Questionable cases were discussed with the board-certified veterinary specialist in diagnostic imaging (S.S.) and a consensus was reached. Observers were not blinded to patient signalment and history. When a smooth or mildly irregular bony double contour at the cranial aspect of the humerus, paralleling the cranial cortex of the bone (HPRLL), was visible, and soft tissue abnormalities or structural changes of the humerus at this level were absent in the radiographs, a grading was conducted according to the following graduation scheme: A HPRLL extending over less than approximately one-quarter of the humerus diaphysis was scored as "focal" (Figure 1A). When HPRLL extended over more than approximately one-quarter of the humerus diaphysis, it was scored as

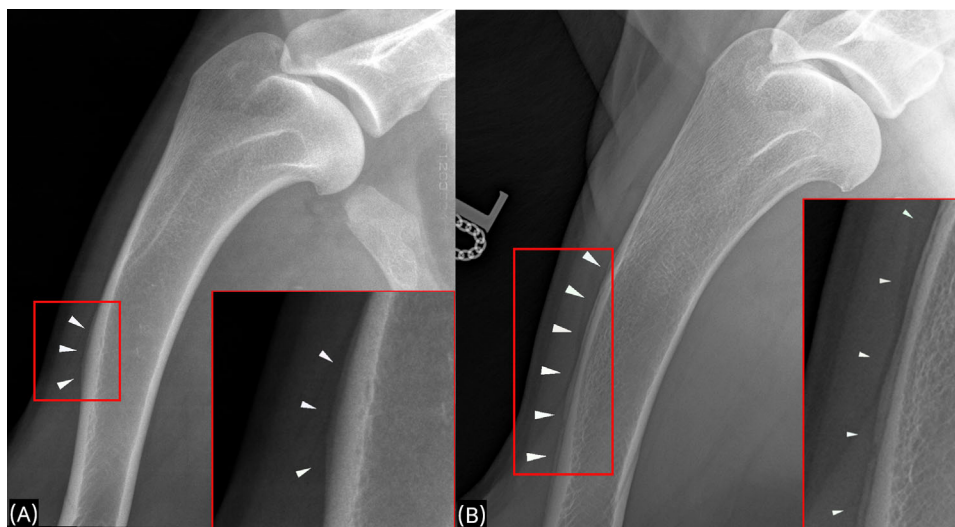


**FIGURE 1** Mediolateral radiographs of the proximal humerus of two dogs with HPRL. A, Focal HPRL in a 6-year-old female German Shepherd dog (arrowheads; 60kVp, 5mAs). B, Extended HPRL in a 7-year-old male Leonberger (arrowheads). 66kVp, 6.3mAs. Zoomed images in the lower right corners, field of view indicated by the red rectangle in Figures A and B [Color figure can be viewed at [wileyonlinelibrary.com](https://onlinelibrary.wiley.com/doi/10.1111/vim.13203)]

“extended” (Figure 1B). To keep the grading scheme simple, no absolute measurements of the HPRL were conducted.

### 2.2.3 | Cadaver specimen analyses

The radiographic findings were evaluated by exemplary anatomical preparation of the cadaver of one dog. The right humerus of a 7-year-old female German Shepherd crossbreed dog with a body weight of 28 kg, euthanized due to a condition unrelated to the musculoskeletal system, was examined. Prior to anatomical preparation, both humeri were radiographed in mediolateral, craniocaudal, medio-caudal to latero-cranial, and medio-cranial to latero-caudal oblique projections (66 kV, 6.3 mAs; Fluorospot Compact FD MultixF-10500, Siemens Healthcare, Erlangen, Germany). Anatomical preparation and examination were performed by M.N. under supervision of a specialist in veterinary anatomy (C.S.). Skin and musculature were carefully dissected to visualize the muscular insertions at the cranial aspect of the humerus. Macroscopic and palpatory findings of the anatomical examination were re-evaluated in mediolateral radiographs of the dissected humerus (60 kV, 5 mAs; Fluorospot Compact FD MultixF-10500, Siemens Healthcare, Erlangen, Germany). After gross anatomical dissection, specimens for histological examination were taken at the level of the HPRL as well as from the sulcus musculi brachialis (control) by use of a diamond-coated, water-cooled micro-band saw (MBS 240/E, Proxxon S.A., Wecker, Luxembourg). Collected specimens were decalcified for two weeks in glass bottles (capacity 10 ml) using buffered ethylenediaminetetraacetate (EDTA), pH 8.0, at room temperature on a platform shaker (Polymax 1040, Heidolph Instruments, Schwabach, Germany). During this time, the EDTA-solution was changed twice a week. Following decalcification, specimens were rinsed using tap water and stored overnight in phosphate-buffered-saline (PBS) (Carl Roth GmbH, Karlsruhe, Germany).

By use of an automatic tissue infiltration machine (JungTP 1050, Leica Biosystems Nussloch GmbH, Nussloch, Germany), the specimens were dehydrated through an ascending alcohol series and embedded in paraffin wax using an automatic embedding system (EG1150h, Leica Biosystems Nussloch GmbH, Nussloch, Germany). Subsequently, 7- $\mu$ m-thin sections were cut on a slide microtome (RM2125RT, Leica Microsystems GmbH, Wetzlar, Germany), dried overnight at 37°C in an incubator (BE 200, Memmert GmbH & Co KG, Schwabach, Germany) and stained with Saffranin-O. Transverse sections of the proximal, middle, and distal humerus diaphysis at the level of the HPRL were microscopically evaluated using light as well as differential interference contrast microscopy (Leica DM2500, Leica Microsystems GmbH, Wetzlar, Germany).

### 2.3 | Statistical analysis

Statistical analysis was performed by a first-year ECVI resident (M.N.) with a course-work training in statistics using commercially available software (IBM® SPSS Statistics version 28, Chicago, Illinois, USA). Age, weight, sex, and breed as well as presence of HPRL were analyzed statistically. Data were assessed for normality using the Shapiro–Wilk test. Unless specified otherwise, the level of significance was set at  $< 0.01$ . All analyses were performed with dog as the unit of analysis. The relationship of age and weight to the presence of an HPRL was investigated by calculation of an eta-coefficient ( $\eta$ ) and eta-square ( $\eta^2$ ). The eta-coefficient and eta-square are used to describe the relationship between a nominal variable and a metric variable and are also used in social sciences.<sup>7–9</sup> According to Cohen,<sup>10</sup>  $\eta^2 < 0.01$  implies a small effect,  $\eta^2 = 0.01–0.06$  implies a medium effect, and  $\eta^2 > 0.06$  implies a large effect of the first variable (age or weight, respectively) on the expression of the second variable (presence of HPRL). Age and weight differences between dogs with and without HPRL were

analyzed using a Mann-Whitney U test. Multivariate logistic regression analyses were performed to assess the strength of association of age and weight with the presence of HPRLL. Furthermore, a chi-square test was used for the analysis of the relationship between breed and sex and the presence of HPRLL (nominal data). Effect size of the chi-square test was calculated using Cramer's V.  $V > 0-0.1$  implies no effect for the statistical correlation of two variables,  $V > 0.1-0.3$  implies a small effect,  $V > 0.3-0.5$  implies a moderate effect, and  $V > 0.5-1$  implies a large effect on the statistical correlation of two variables.<sup>10</sup>

### 3 | RESULTS

#### 3.1 | Dogs

The automatic search for radiographs yielded 3214 dogs with mediolateral radiographs of one or both humeri and 1727 dogs met the inclusion criteria. Mediolateral radiographs of the humerus or shoulder joint were acquired with one of three radiographic systems (PCR eleva, Philipps medical systems, Best, Netherlands; Console Advance DR-ID 300 CL, Fujifilm medical systems, Stamford, USA; or Fluorospot Compact FD MultixF-10500, Siemens Healthcare, Erlangen, Germany). Standard exposure values adapted to the patient size and a film-focus distance of 100–115 cm were used. Both humeri were reviewed in 1150 dogs (66.6%), only the right humerus in 308 dogs (17.8%), and only the left humerus in 269 dogs (15.6%), thus 2877 humeri were included.

The breeds most frequently represented in the study population were mixed breeds (377, 21.8%), Labrador Retrievers (268, 15.5%), German Shepherd dogs (112, 6.5%), Golden Retrievers (68, 3.9%), Bernese Mountain dogs (59, 3.4%), Rottweilers (53, 3.1%), Border Collies (38, 2.2%), Australian Shepherds (35, 2.0%), Rhodesian Ridgebacks (33, 1.9%), Boxers (32, 1.9%), English Bulldogs (24, 1.4%), French Bulldogs (23, 1.3%), Great Swiss Mountain dogs (21, 1.2%), Hovawarts (21, 1.2%), German Wirehaired Pointers (20, 1.2%), and several other breeds of various sizes with an average of four representatives each (Appendix 1). At the time of the X-ray examination, the study population had an average age of  $4.4 \pm 3.9$  years (0–20 years). Overall 68.5% of the dogs were < 7 years of age and 31.5% were  $\geq 7$  years of age. The mean body weight was  $29.0 \pm 13.1$  kg (0.5–89.0 kg), with 52.6% of the dogs weighing < 30 kg and 47.4% of the dogs weighing  $\geq 30$  kg. The average age and weight per breed are depicted in Appendix 1. Overall, 669 males (38.7%), 324 neutered males (18.8%), 413 females (23.9%), and 321 spayed females (18.6%) were included.

#### 3.2 | Radiographic analyses

For the 1727 dogs meeting study inclusion criteria, 387 had HPRLL (prevalence 22.4%). The lesion was not visible in craniocaudal or caudocranial projections. In 264 of the dogs with HPRLL, both humeri were radiographed and a HPRLL was present bilaterally in 255 dogs (96.6%

of dogs with bilateral radiographs, 65.9% of all dogs with HPRLL). In the remaining 123 dogs with HPRLL with only one humerus depicted, the right humerus showed HPRLL in 73 dogs (18.6%), the left humerus in 60 dogs (15.5%), resulting in a total of 643 humeri in 387 dogs with a HPRLL. A focal HPRLL was present in 248 dogs (64.1%) and an extended HPRLL was visible in 139 dogs (35.9%) (for examples see Figure 1A and 1B). All dogs radiographed bilaterally showed either focal or extended HPRLL on both sides, none of the dogs had focal changes on one and extended changes on the other side. In general, the visibility of HPRLL subjectively varied between different x-ray machines used.

#### 3.3 | Statistical analyses

A comparison of age, body weight, and sex for dogs with and without HPRLL is provided in Table 1. A higher body weight had a medium, almost large, statistically significant effect on the presence of HPRLL ( $P < 0.001$ ;  $\eta = 0.365$ ,  $\eta^2 = 0.133$ ) Dogs weighing  $\geq 30$  kg more often showed HPRLL than smaller breed dogs ( $P < 0.001$ , Cramer's  $V = 0.32$ ). Logistic regression analysis showed a positive effect of increasing body weight on the presence of HPRLL (odds ratio: 1.077, 95% confidence interval: 1.066–1.089,  $P < 0.001$ ). Figure 2 shows the increased frequency of dogs with HPRLL with increasing body weight. HPRLL was visible in only two dogs (1.3%) weighing less than 10 kg, both were focal.

Dogs with HPRLL had a statistically significant higher age and weight compared to dogs without HPRLL ( $P < 0.001$ , Table 1). Higher age had a medium, but statistically significant effect on the presence of HPRLL ( $P < 0.001$ ;  $\eta$  coefficient = 0.292,  $\eta^2 = 0.085$ ). According

**TABLE 1** Clinical characteristics of dogs with and without HPRLL

|   | Dogs with HPRLL      | Dogs without HPRLL   |
|---|----------------------|----------------------|
| age   |                      |                      |
| average age $\pm$ standard deviation (range) in years | $6.5 \pm 3.1$ (1-20) | $3.7 \pm 3.9$ (0-16) |
| <7 years (dog number and %)                           | 186 (48.1%)          | 998 (74.5%)          |
| $\geq 7$ years (dog number and %)                     | 201 (51.9%)          | 342 (25.5%)          |
| body weight   |                      |                      |
| average body weight $\pm$ standard deviation in kg    | $37.9 \pm 12.7$      | $26.5 \pm 12.1$      |
| <30 kg (dog number and %)                             | 88 (22.7%)           | 820 (61.2%)          |
| $\geq 30$ kg (dog number and %)                       | 299 (77.3%)          | 520 (38.8%)          |
| Sex   |                      |                      |
| Males (dog number and %)                              | 146 (37.7%)          | 523 (39.0%)          |
| Neutered males (dog number and %)                     | 80 (20.7%)           | 244 (18.2%)          |
| Females (dog number and %)                            | 51 (13.2%)           | 362 (27.0%)          |
| Spayed females (dog number and %)                     | 110 (28.4%)          | 211 (15.7%)          |

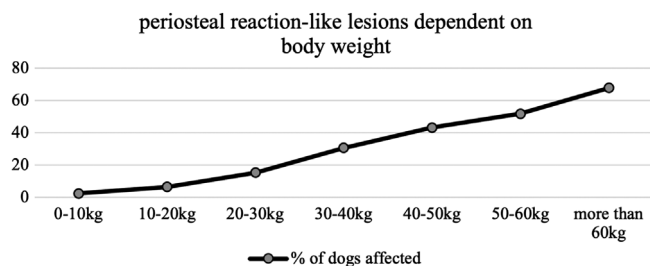


**FIGURE 2** Radiographic visibility of HPRL in different weight groups in percent. Weight groups are plotted on the x-axis and % of dogs with HPRL within these weight groups are plotted on the y-axis

to logistic regression analysis, increasing age had a positive effect on the presence of HPRL (odds ratio: 1.19, 95% confidence interval: 1.1–1.2,  $P < 0.001$ ). Dogs  $\geq 7$  years of age were more frequently affected than younger dogs ( $P < 0.001$ , Cramer's  $V = 0.24$ ). HPRL were most commonly visible in the group of 7–9-year-old dogs (139/332, 41.9%, average weight: 31.8 kg). In the group of dogs aged 10–12 years and more than 12 years, the prevalence of HPRL was comparable to the group of 4–6-year-old dogs (Figure 3). The average weight in the group of dogs with 4–6 years was 30.4 kg, in dogs aged 10–12 years, the average weight was 26.4 kg. The chi-square test for evaluating the effect of sex on the presence of HPRL revealed a statistically significant difference between the sexes with spayed females being overrepresented ( $P < 0.001$ ; Cramer's  $V = 0.135$ ) and intact females being underrepresented ( $P < 0.001$ ; Cramer's  $V = 0.136$ ) compared to intact males ( $P = 0.643$ ) and neutered males ( $P = 0.259$ ).

The majority of dogs with HPRL (> 10 individuals) were mixed breed dogs, Labrador Retrievers, German Shepherd dogs, Rottweilers, Bernese Mountain dogs, Golden Retrievers, Newfoundlands, and Rhodesian Ridgebacks. Various other breeds were represented by less than 10 dogs each (Appendix 1). A statistical comparison of the dog breeds was conducted when at least 51 breed representatives were included (confidence interval 85%), thus mixed breeds, Labrador Retrievers, German Shepherd dogs, Golden Retrievers, Bernese Mountain dogs, and Rottweilers were evaluated statistically. German Shepherd dogs and Rottweilers significantly more often showed HPRL than other breeds ( $P < 0.01$ ) and affiliation to one of these breeds had a small effect on the presence of HPRL according to Cramer's  $V$  (Table 2). Unfortunately, only small numbers of large and giant breed dogs were represented in the study population, hindering statistical evaluation of these breeds. For example, 12 Newfoundlands were included in our study population and 11 of these (92%) showed focal or extended HPRL. Similarly, eight of 12 Leonbergers (67%), six of 12 Dogues de Bordeaux (50%), and three of nine Great Danes (33%) had HPRL (Appendix 1).

### 3.4 | Cadaver specimen analyses

Mediolateral, craniocaudal, and oblique radiographs of both humeri of the cadaver prior to anatomical preparation were acquired. Bilat-

**TABLE 2** Chi-square test regarding the effect of breed on the presence of HPRL

| Breed                | P-value | Cramer's V |
|----------------------|---------|------------|
| Bernese Mountain dog | 0.572   | 0.014      |
| German Shepherd dog  | <0.001* | 0.112      |
| Golden Retriever     | 0.944   | 0.002      |
| Labrador Retriever   | 0.866   | 0.004      |
| Mixed breed          | 0.185   | 0.032      |
| Rottweiler           | <0.001* | 0.154      |

Cramer's  $V > 0-0.1$ : no effect;  $V > 0.1-0.3$ : small effect,  $V > 0.3-0.5$  moderate effect,  $V > 0.5-1$  large effect on the statistical correlation of two variables<sup>10</sup>.

eral, extended HPRL were visible on the mediolateral radiographs (Figure 4A). Pronation of the forelimb (oblique medio-cranial to latero-caudal projection) led to an increased visibility of the HPRL at the cranial aspect of the mid-third of the humeral diaphysis and the lesion was no longer visible at the proximal third of the diaphysis (Figure 4B). Supination (oblique medio-caudal to latero-cranial projection) led to increased visibility of the lesion in the proximal third of the humeral diaphysis and the lesion was no longer visible in the mid-third of the humerus diaphysis (Figure 4C).

After resection of the skin and adipose tissue, the muscular insertions at the humerus were visualized. The pectoralis musculature was visualized spanning between the sternum and the cranial aspect of the humerus (Figure 5A). Both parts of the Mm. pectorales superficiales, i.e. the M. pectoralis descendens and the M. pectoralis transversus, were identified with moderate separation from each other. The origin of the Mm. pectorales superficiales at the cranial part of the sternum was identified. The muscle extended laterally to the cranial aspect of the humerus, covering the M. biceps brachii on its craniomedial side. The entheses of the Mm. pectorales superficiales was visualized and palpated along the cranial aspect of the humerus diaphysis (Figure 5B). Alongside the attachment of the Mm. pectorales superficiales, a flat bony ridge (< 1 mm) with a proximodistal course was palpable.

After exarticulation of the right forelimb, the mediolateral radiograph of the right humerus was repeated (Figure 6A). At the level of the entheses of the Mm. pectorales superficiales to the humerus, a window with a width of 10 mm was cut out deeply to the bone with a scalpel. The radiograph was then repeated and an interruption of the previously visualized HPRL was apparent (Figure 6B, C).

In the histological examination of the transverse slices of the humerus at the level of the HPRL, no abnormalities of the bone or periosteum were found. At the level of the HPRL, a flat ridge of lamellar bone with a moderately undulating contour of the surface was visible (Figure 7A). At the level of the attachment of the skeletal musculature to the bone, a fibrocartilaginous entheses was identified with collagenous fiber bundles in parallel arrangement and interposed rows of chondrocytes parallel to the direction of the fibers. The orientation of the fiber bundles was perpendicular to the bone surface (Figure 7B).

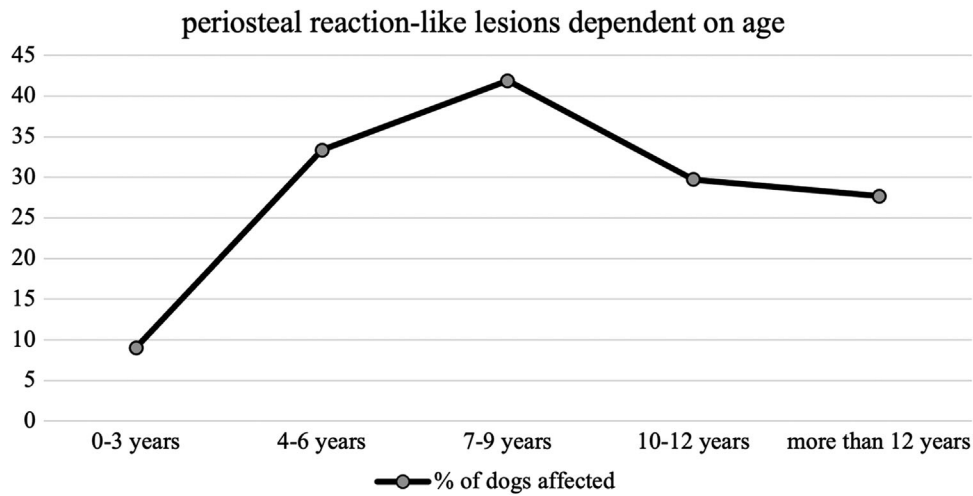


**FIGURE 3** Radiographic visibility of HPRLI in different age groups. Age groups are plotted on the x-axis and % of dogs with HPRLI within these age groups are plotted on the y-axis

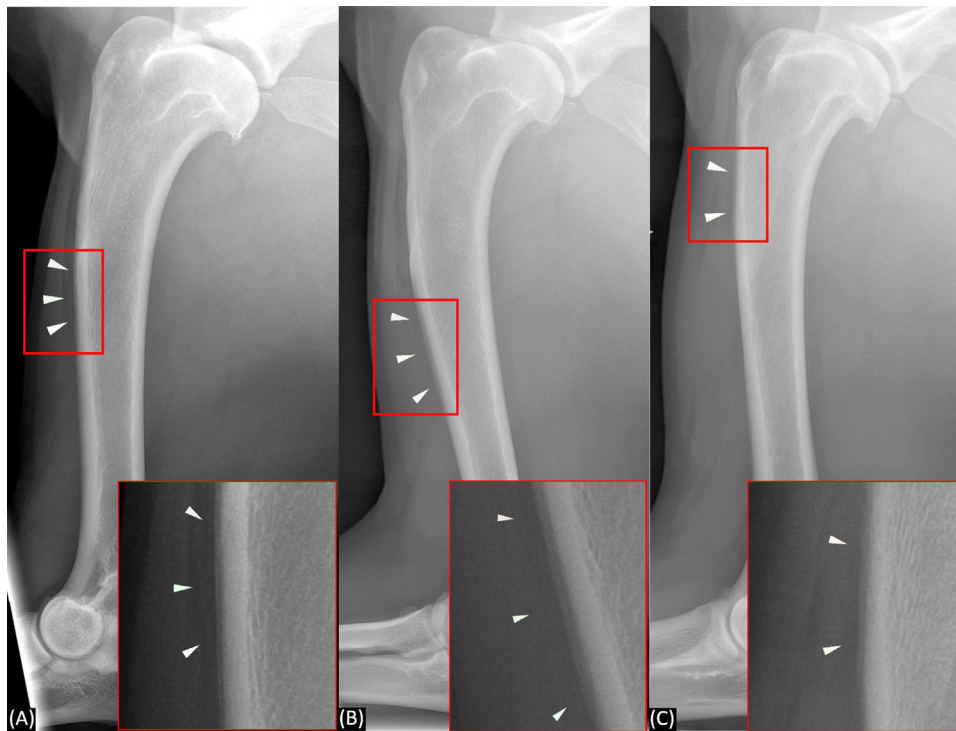


**FIGURE 4** Mediobasal radiographs prior to dissection of the humerus of a 7-year-old female German Shepherd dog that underwent anatomical preparation of the right humerus. A, Neutral mediobasal radiograph with extended HPRLI (arrowheads). B, Oblique medio-cranial to latero-caudal radiograph (pronation) with HPRLI visible more distally compared to A (arrowheads). C, Oblique medio-caudal to latero-cranial radiograph (supination) with HPRLI visible more proximally compared to A (arrowheads). Zoomed images in the lower right corners, field of view indicated by the red rectangle in Figures A, B and C. (66kVp, 6.3mAs) [Color figure can be viewed at [wileyonlinelibrary.com](http://wileyonlinelibrary.com)]

## 4 | DISCUSSION

Findings supported our hypotheses that lamellar periosteal reaction-like lesions at the cranial aspect of the middle and proximal humeral diaphysis have a high prevalence in older, large breed dogs in medi-

olateral radiographs including parts of the humerus and were not associated with clinical complaints or underlying pathology. According to our anatomical and histological examination of one canine cadaver, HPRLI represented the attachment site of the Mm. pectorales superficiales to the humerus, consisting of a fibrocartilaginous enthesis to the



**FIGURE 5** Anatomical preparation of the right forelimb of a 7-year-old female German Shepherd dog, dorsal recumbency. A, Craniomedioventral view of the right forelimb. 1: M. pectoralis descendens, 2: Mm. pectorales superficiales, 3: M. brachiocephalicus, 4: M. deltoideus, 5: M. biceps brachii (dissected), 6: M. brachialis (dissected). B, Caudomedial view after dissection of the M. pectoralis superficialis (held by forceps). Insertion of the Mm. pectorales superficiales along the cranial aspect of the humerus diaphysis (arrows) [Color figure can be viewed at [wileyonlinelibrary.com](https://onlinelibrary.wiley.com)]

Crista tuberculi majoris and Crista humeri. These structures have not yet been described as being visible in mediolateral radiographs of the humerus in dogs. In anatomy textbooks, the Crista tuberculi majoris is described at the cranial surface of the humerus, passing medially to the deltoid tuberosity, reaching the cranial edge of the brachialis groove distally, bordered by the Crista humeri.<sup>11,12</sup> This course of the Crista tuberculi majoris is reflected in our oblique projections in pronation and supination of the forelimb. The oblique projections additionally prove the ridge-like appearance of the Crista tuberculi majoris, continued as the Crista humeri, rather than a planar distribution of an actual periosteal reaction. None of the dogs in our study was painful on palpation of the cranial aspect of the humerus diaphysis. In the histological examination, we could neither detect periosteal reactions nor any other pathologic alterations of the humerus. The authors therefore propose that HPRLL is a physiological anatomical structure unrelated to pathological changes and recommend that this should not be mistaken as an aggressive bone lesion.

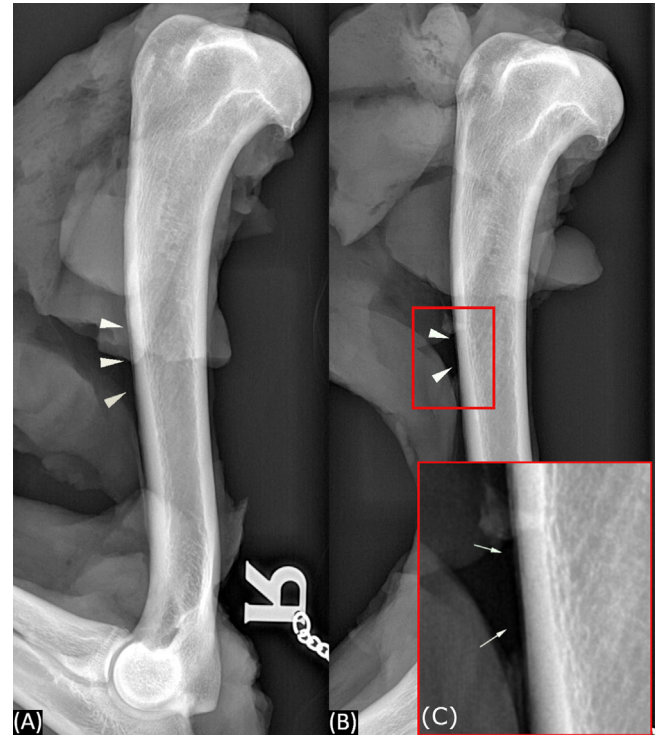


**FIGURE 6** Mediolateral radiographs of the right humerus after anatomical preparation, same dog as in Figure 4 and 5. A, Focal HPRLL is still visible after anatomical preparation (arrowheads). B, After resection of 1 cm of the attachment of the Mm. pectorales superficiales deep to the bone, there is a discontinuity visible in the HPRLL (arrowheads in ). The rectangle indicates the field of view provided in C. C, Magnification of the resection site of the HPRLL (arrows). (60kVp, 5mAs) [Color figure can be viewed at [wileyonlinelibrary.com](https://onlinelibrary.wiley.com)]

Tendons are attached to bone by connective tissue in the form of a fibrous or fibrocartilaginous enthesis.<sup>13</sup> Fibrocartilaginous entheses can be distinguished in four zones.<sup>14,15</sup> The first zone represents the end of the tendon, composed of parallel collagen bundles, the second zone consists of unmineralized fibrocartilage. Mineralization is a physiological process in the development of fibrocartilaginous entheses, as the third zone of the normal fibrocartilaginous enthesis contains mineralized fibrocartilage and the fourth zone consists of trabecular bone.<sup>14,15</sup> Fibrocartilage develops in normal entheses as a response to compression.<sup>13</sup> The collagen fibers in the fibrocartilage provide a unique flexibility and function as a stress protector to the tendon, whereas the mineralized zone protects the bone.<sup>13,16,17</sup> According to the importance and main direction of the local forces, the thickness of the fibrocartilage varies<sup>13,18</sup> as well as the thickness of the zone of calcified fibrocartilage, related to the physiological strength and loading of the tendon.<sup>19</sup> Furthermore, mechanical load is crucial for the development of bony tubercles at the level of entheses.<sup>20,21</sup> Various growth factors like TGF $\beta$  and BMP for the initiation of growth and IHH/PTHrP for the maturation and mineralization of muscle–tendon attachments have been identified in human beings.<sup>20</sup> In our histological examination, we detected a physiological fibrocartilaginous enthesis at the level of the attachment of the Mm. pectorales superficiales to the

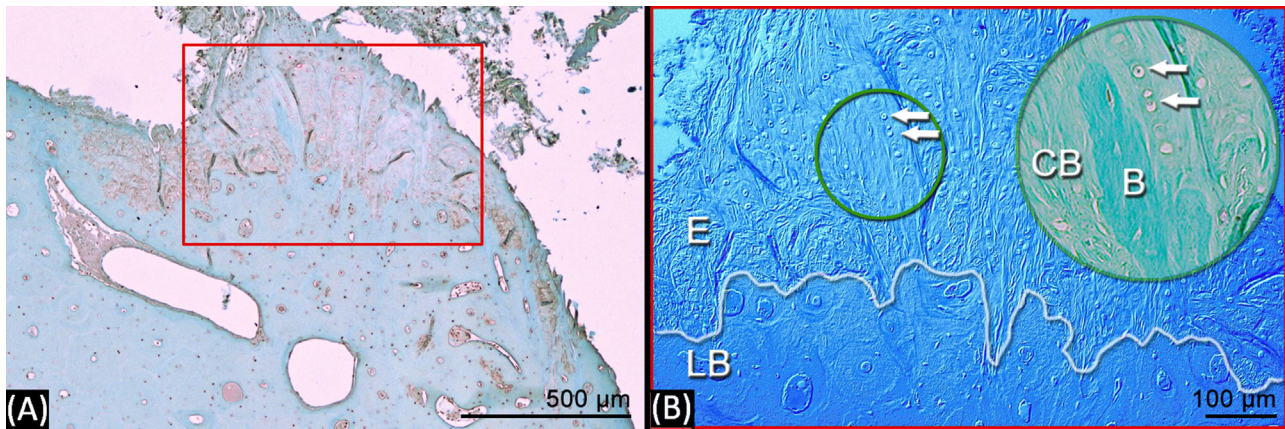


**FIGURE 7** Histological sections of the enthesis of the Mm. pectorales superficiales, decalcified specimens, paraffin wax embedding, Safranin-O-stain. A, Overview (light microscopy) showing the protuberant shape of the enthesis. The rectangle indicates the field of view provided in B. B, Differential interference contrast microscopy enhancing the different structural components of the enthesis. The lamellar bone (LB) of the humerus is separated from the enthesis (E) by an undulating interface (white line). Inset, light microscopy. The enthesis is composed of a mixture of collagen fiber bundles (CB), fibrocartilaginous elements (indicated by a typical lining of chondrocytes, arrows), and bony structures (B) [Color figure can be viewed at [wileyonlinelibrary.com](http://wileyonlinelibrary.com)]

Crista tuberculi majoris and Crista humeri. Due to decalcification of the slices, we are unable to comment on the degree of mineralization of the fibrocartilage at the attachment site. Thus, it remains unclear whether the radiographically visible HPRLL only resembles an exaggerated bony Crista tuberculi majoris and Crista humeri or whether the mineralized fibrocartilage of the enthesis is also visible radiographically. Heterogenous mineralization of the fibrocartilage could explain the mildly irregular appearance of the HPRLL in the radiographs, but also the irregularity of the bony surface of the Crista tuberculi majoris and Crista humeri, visible in our histological examination, can explain this appearance.

Biomechanical studies of the forelimb musculature in dogs prove the activity of the Mm. pectorales superficiales during protraction of the humerus in the second half of the stance phase, during deceleration in a forward direction as well as in stabilization of the limb against abducting forces.<sup>22–24</sup> In our study, higher body weight of the patients was associated with a higher prevalence of HPRLL. Furthermore, we found a higher prevalence of HPRLL in Rottweilers, which have a compact body conformation and high muscle volume. This finding is consistent with the demanding biomechanical forces transferred to the bone in muscular dogs and subsequent remodeling of the enthesis described previously. The second breed showing HPRLL more commonly than other breeds was the German Shepherd dog. Breeds with a body mass comparable to German Shepherd dogs like Golden or Labrador Retrievers were not overrepresented. The average age of the German Shepherd dogs was 4.0 years, the age of the Rottweilers and Golden Retrievers 3.6 years, and 3.8 years in the Labrador Retrievers. Therefore, we assume that age is not the main factor for the varying visibility of HPRLL in this breed. Breed-specific physical activity and sportive utilization with resulting biomechanical demands to the entheses may further explain the breed dispositions of German Shepherds and Rottweilers. Due to the retrospective character of our study, information about physical activity was not constantly available in the medical reports and the effect cannot be evaluated. Unfortunately, only a small

number of giant dog breeds was represented in our study population. Although not statistically evaluable due to the small group size, our data indicate a very high prevalence of HPRLL in Newfoundlands, Leonbergers, and Dogues de Bordeaux. Among chondrodystrophic breeds, only the Dachshund (2/8 dogs) and the Shih Tzu (1/3) showed HPRLL, while none of the French Bulldogs (0/23), Jack Russel terriers (0/9), or Welsh Corgi Cardigans (0/1) showed HPRLL. However, chondrodystrophic dog breeds were underrepresented in our population and thus, we cannot assume or rule out a breed predisposition. Comparative biomechanical and electromyographic data of the pectoral muscle activity of different dog breeds and body conformation is not available, but could potentially reveal different mechanical loads to the bone and further prove our hypotheses.

Age was another factor affecting the presence of HPRLL, as dogs  $\geq 7$  years were overrepresented in the group with HPRLL. The prevalence within the group of dogs of 10–12 years and older than 12 years was almost equal to the group of 4–6 years. This finding can be explained by the breed and weight distribution among the age groups. In the group of dogs older than 10 years, the average weight of dogs was 25.6 kg, in the group of all dogs with HPRLL, the average weight was 37.9 kg. Smaller dog breeds are known to have a higher life expectancy than large dog breeds, which explains the higher number of smaller dogs with higher ages and in contrast, reduced prevalence of HPRLL in this age group. In a rat-model study, an increased mineralized zone and decreased non-mineralized zone of the enthesis was found in aging rotator-cuff entheses.<sup>25</sup> Although comparable studies in dogs are lacking, age-related increased mineralization of the entheses could have increased the radiographic visibility of the entheses in older dogs in our study. Other degenerative changes of the enthesis, accompanied by calcifying metaplasia, is another potential explanation for the radiographic visibility of the enthesis. However, in our histological examination of one middle-aged dog, no degeneration of the enthesis of the Mm. pectorales superficiales was apparent.

Among the dogs with HPRL, spayed females are significantly overrepresented. Exact determination of the effect of sex and neutering/spaying on the visibility of the enthesis of the Mm. pectorales superficiales was not possible and beyond the scope of this study and requires further investigation. An incidental overrepresentation of spayed females, as the smallest sex group included, is possible.

This study has some limitations. First, the retrospective character prevents optimal comparison between the breed and age groups, thus evaluation of the prevalence of HPRL in giant breeds was limited. Three different x-ray machines with different recording parameters and algorithms were utilized, thus technical parameters may have affected the visibility of slight mineralization. Subjectively assessed, the visibility of HPRL differed between the machines, although all radiographs included were classified as diagnostic. Furthermore, our study population mostly represents the spectrum of patients presented to our clinic due to front limb lameness. As a part of the internal standard operating procedure in dogs with suspected elbow dysplasia, radiographs of the elbow and shoulder joints are acquired in these patients. This procedure potentially decreased the average age of the study population. Furthermore, front limb lameness is more common in large breed dogs due to higher prevalence of osteochondrosis, elbow dysplasia, panosteitis, or bone neoplasia and thus may have increased the average weight and patient number of certain breeds within the study population. Second, we were unable to perform sampling of the HPRL in the dogs. Based on the medical reports, diaphyseal pain of the humerus was not present in any of the dogs. The only histological examination performed in this study revealed an unremarkable structure of the enthesis of the Mm. pectorales superficiales and underlying bone. Nevertheless, a pathology of the enthesis, periosteum, bone, or surrounding soft tissue structures cannot be ruled out in all cases. Third, the reviewers were not blinded to the signalment of the dogs, which could have led to a certain bias in detection of HPRL in questionable cases.

In conclusion, HPRL at the cranial aspect of the humeral diaphysis has a high prevalence in older, large breed dogs and may represent the attachment of the Mm. pectorales superficiales via a fibrocartilaginous enthesis to the humerus. The authors alert veterinarians not to overinterpret the findings as aggressive bone disease. In questionable cases or pain related to the cranial aspect of the humerus and no other clinical or radiographic findings detectable, we recommend bone biopsies to rule out early states of underlying pathology. Further research concerning the underlying remodeling processes of the enthesis in the context of biomechanical properties of the inserting musculature are encouraged.

## ACKNOWLEDGMENTS

The authors would like to acknowledge Jörg Vogelsberg and Jutta Dern-Wieloch for their assistance in preparation of the histological sections.

## LIST OF AUTHOR CONTRIBUTIONS

### Category 1

- (a) Conception and Design: Nickel, Schikowski, Staszky, Schaub
- (b) Acquisition of Data: Nickel, Schikowski
- (c) Analysis and Interpretation of Data: Nickel, Schikowski, Staszky, Schaub

### Category 2

- (a) Drafting the Article: Nickel, Schikowski
- (b) (b) Revising Article for Intellectual Content: Staszky, Schaub

### Category 3

- (a) Final Approval of the Completed Article: Nickel, Schikowski, Staszky, Schaub

### Category 4

- (a) Agreement to be accountable for all aspects of the work in ensuring that questions related to the accuracy or integrity of any part of the work are appropriately investigated and resolved: Nickel, Schikowski, Staszky, Schaub

## CONFLICT OF INTEREST

The authors have declared no conflicts of interest.

## PREVIOUS PRESENTATION DISCLOSURE

The study findings have not been reported in any previous scientific meeting.

## REPORTING GUIDELINE DISCLOSURE

No EQUATOR network or other reporting guideline checklist was used.

## DATA AVAILABILITY STATEMENT

The raw data supporting the conclusions of this article will be made available by the authors, without undue reservation.

## ORCID

Mareike-Kristin Nickel  <https://orcid.org/0000-0003-4361-6713>

## REFERENCES

1. Burt JK, Wilson GP. A study of eosinophilic panosteitis (Enostosis) in German Shepherd dogs. *Acta Radiol. Diagn.* 1972;13:7-13. <https://doi.org/10.1177/0284185172013S31903>
2. Davis GJ, Kapatkin AS, Craig LE, Heins GS, Wortman JA. Comparison of radiography, computed tomography, and magnetic resonance imaging for evaluation of appendicular osteosarcoma in dogs. *J Am Vet Med Assoc*;220:1171-1176. Accessed January 2022. <https://avmajournals.avma.org/view/journals/javma/220/8/javma.2002.220.1171.xml>
3. Wallack S, Wisner E, Werner J, et al. Accuracy of magnetic resonance imaging for estimating intramedullary osteosarcoma extent in pre-operative planning of canine limb-salvage procedures. *Vet Radiol Ultrasound.* 2002;43:432-441.
4. Kirberger RM, McEvoy FJ. *BSAVA Manual of Canine and Feline Musculoskeletal Imaging.* Wiley; 2016;75-86.

5. Ruth D, Kirberger RM, Barr F, Wrigley RH. *Handbook of Small Animal Radiology and Ultrasound*. W.B. Saunders; 2010;1-37. Accessed January 2022. <https://www.sciencedirect.com/science/article/pii/B9780702028946000019>
6. Kealy JK, McAllister H, Graham JP. Diagnostic Radiology and Ultrasonography of the Dog and Cat. *Saunders*. 2011; 351-446. Accessed January 2022. <https://books.google.de/books?id=IJ18JULz9mMC>
7. Benninghaus H. *Die Beschreibung der Beziehung zwischen einer nominalen und einer metrischen Variablen*. Wiesbaden: VS Verlag für Sozialwissenschaften; 2007;228-249. Available from: [https://doi.org/10.1007/978-3-531-90739-0\\_8](https://doi.org/10.1007/978-3-531-90739-0_8)
8. Pearson KI. Mathematical contributions to the theory of evolution.—XI. On the influence of natural selection on the variability and correlation of organs. *Phil Trans R Soc*. 1903;200:1-66.
9. Pearson K. *On the general theory of skew correlation and non-linear regression*. Dulau & Co.; 1905;
10. Cohen J. *Statistical Power Analysis for the Behavioral Sciences*. Taylor & Francis; 1988; Accessed January 2022. <https://books.google.de/books?id=cJH0IR33bgC>. Available from.
11. Frewein J, Nickel R, Schummer A, Seiferle E. *Lehrbuch der Anatomie der Haustiere: Bewegungsapparat*. Parey; 2001;79-83. Accessed January 2022. <https://books.google.de/books?id=mN4kPwAACAAJ>. Available from.
12. Evans HE, Lahunta Ade. *Miller's Anatomy of the Dog*. Saunders; 2013;233-254. Accessed January 2022. <https://books.google.de/books?id=6eBOAQAQBAJ>
13. Benjamin M, Ralphs J. Fibrocartilage in tendons and ligaments—an adaptation to compressive load. *J Anat*. 1998;193:481-494.
14. Cooper RR, Misol S. Tendon and ligament insertion. A light and electron microscopic study. *The Journal of bone and joint surgery American volume*. 1970;52(1):1-20.
15. Rufai A, Ralphs J, Benjamin M. Structure and histopathology of the insertional region of the human achilles tendon. *J Orthop Res*. 1995;13:585-593. <https://doi.org/10.1002/jor.1100130414>. Available from.
16. Claudepierre P, Voisin M-C. The entheses: histology, pathology, and pathophysiology. *Joint Bone Spine*. 2005;72:32-37. Accessed January 2022. <https://www.sciencedirect.com/science/article/pii/S1297319x04000739>
17. Hannes S. Zur Struktur der Sehnenansatzzonen. *Zeitschrift für Anatomie und Entwicklungsgeschichte*. 1956;119:431-456. <https://doi.org/10.1007/BF00522699>
18. Matyas J, Anton M, Shrive N, Frank C. Stress governs tissue phenotype at the femoral insertion of the rabbit MCL. *J Biomech*. 1995;28:147-157. Accessed January 2022. <https://www.sciencedirect.com/science/article/pii/S002192909400058C>
19. Gao J, K M. Quantitative comparison of soft tissue-bone interface at chondral ligament insertions in the rabbit knee joint. *J Anat*. 1996;188(2):367-373. Accessed January 2022. <https://pubmed.ncbi.nlm.nih.gov/8621336>
20. Zelzer E, Blitz E, Killian ML, Thomopoulos S. Tendon-to-bone attachment: from development to maturity. *Birth Defects Res C Embryo Today*. 2014;102:101-112. Accessed January 2022. <https://pubmed.ncbi.nlm.nih.gov/24677726>
21. Tatara AM, Lipner JH, Das R, et al. The role of muscle loading on bone (Re)modeling at the developing enthesis. *PLoS One*. 2014;9:e97375-e97375. Accessed January 2022. <https://pubmed.ncbi.nlm.nih.gov/24847982>
22. Carrier DR, Deban SM, Fischbein T. Locomotor function of forelimb protractor and retractor muscles of dogs:evidence of strut-like behavior at the shoulder. *J Exp Biol*. 2008;211:150-162. <https://doi.org/10.1242/jeb.010678>
23. Emanuel A, Reinhardt L, Lucas K, Fischer M. Three-dimensional inverse dynamics of the forelimb of Beagles at a walk and trot. *Am J Vet Res*. 2017;78:804-817. Accessed January 2022. <https://avmajournals.avma.org/view/journals/ajvr/78/7/ajvr.78.7.804.xml>
24. Tokuriki M. Electromyographic and joint-mechanical studies in quadrupedal locomotion: il. *Trot Japanese Journal of Veterinary Science*. 1973;35:525-533\_2.
25. Zeling L, Nakagawa K, Wang Z, Amadio P, Zhao C, Gingery A. Age-related cellular and microstructural changes in the rotator cuff enthesis. *J Orthop Res*. 2021;n/a:1-13. <https://doi.org/10.1002/jor.25211>

#### SUPPORTING INFORMATION

Additional supporting information can be found online in the Supporting Information section at the end of this article.

**How to cite this article:** Nickel M-K, Schikowski L, Staszuk C, Schaub S. Periosteal reaction-like lesions at the cranial aspect of the humeral diaphysis have a high prevalence in older, large breed dogs and may represent entheses of the superficial pectoral muscles. *Vet Radiol Ultrasound*. 2023;64:368–377. <https://doi.org/10.1111/vru.13203>